Available online at www.sciencedirect.com
SCIENCE DIRECT®

Nuclear Instruments and Methods in Physics Research A 505 (2003) 347–351

NUCLEAR INSTRUMENTS & METHODS IN PHYSICS RESEARCH
Section A

www.elsevier.com/locate/nima

# Real time digital pulse shaper with variable weighting function

Valentin T. Jordanov*

*Canberra Industries, Meriden, CT 06450, USA*

**Abstract**

Real time digital pulse shaper has been developed that provides digital control of the synthesized weighting function (WF). The shaper can synthesize in real time shapes that are optimum or near optimum in the presence of $1/f$ noise. Other pulse shapes including trapezoidal and triangular can be realized. The WF is synthesized by algebraically adding a concave and a convex pulse shapes. The shaper is implemented in a single chip and is a part of a spectroscopy system on a programmable chip.


*PACS:* 29.30.−h; 29.30.Kv

*Keywords:* Digital shaper; $1/f$ noise; Pulse-shaping; Radiation detector; Concave; Convex

## 1. Introduction

Real time digital pulse shaping techniques allow synthesis of pulse shapes that have been difficult to realize using the traditional analog methods. Using digital shapers, triangular/trapezoidal filters can be realized in real time [1,2]. The trapezoidal weighting function (WF) represents the optimum time-limited pulse shape when only parallel and series noise sources are present in the detector system [3–5]. In the presence of $1/f$ noise, the optimum WF changes depending on the $1/f$ noise contribution. Optimum pulse shapes have been derived for both cases of $1/f$ voltage and $1/f$ current noise sources [5,6].

This paper describes a technique to synthesize pulse shapes with variable weighting function (VWF) that can be adjusted for optimal noise suppression at various noise distributions.[1]

## 2. Digital shaper configuration

Fig. 1 shows a simplified diagram of the digital shaper with VWF. This configuration represents a linear, time invariant digital filter. The shaper uses two digital filter modules connected in series.

The first module (Analog Response Removal unit—ARR) unfolds the known responses of the analog pulse processor preceding the ADC. For example, this could be a simple digital differentiator if the analog pulse processor response is a step function (reset type charge sensitive preamplifier). More complex algorithms are executed by ARR when analog low pass filter precedes the sampling ADC [7]. In any case the output of the ARR

*Corresponding author. Address for correspondence: Yantra, 12 Cutts Road, Durham, NH 03824, USA. Tel.: +1-603-868-5404.

*E-mail address:* jordanov@ieee.org (V.T. Jordanov).

[1] Patent Pending.

0168-9002/03/$ - see front matter 
doi:10.1016/S0168-9002(03)01094-5

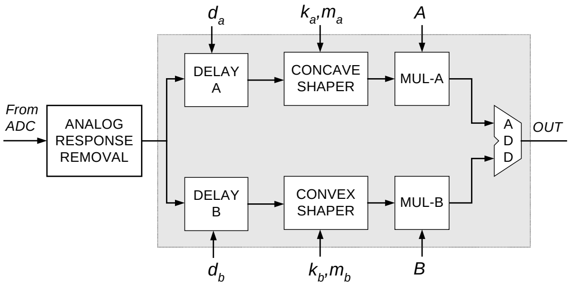


Fig. 1. Simplified diagram of the digital shaper with VWF.

closely represents the signal from the detector—a very short pulse. If the analog response is removed (in reality reduced to a very short pulse) then the digital pulse shaper can be synthesized by simply finding an impulse response that produces the optimal WF. In other words, the main goal is to determine a digital filter with impulse response that matches the optimal WF. Once the WF is synthesized it is possible to combine the ARR function with the WF response in order to achieve more efficient algorithms.

The second module of the digital shaper with VWF is a digital filter that synthesizes the WF. This filter has two parallel chains. The first chain (chain "A") consists of a programmable digital delay line (DELAY-A), digital filter with adjustable rise/fall time and flattop (CONCAVE SHAPER), and digital multiplier (MUL-A). The second chain has functionally the same delay line (DELAY-B) and multiplier (MUL-B). The digital filter (CONVEX SHAPER) has similar controls as the CONCAVE SHAPER but differs in the impulse response. Both chains are fed by the output of the ARR. The multipliers function as gain units while the delay lines provide a mean to align (relative delay) impulse responses of the filter chains. The order of the blocks in each of the chains has no influence on the overall response of the WF filter because each chain represents a linear, time-invariant filter. The output signals of the two chains are summed together by the digital adder (ADD).

The key elements of the VWF digital filter are the CONCAVE and CONVEX shapers. Fig. 2 depicts typical unit impulse responses of these shapers. The responses of the CONCAVE and CONVEX shapers are symmetrical with rise/fall time equal to $k_a$ and $k_b$, respectively. The adjustable flat top portions of the waveforms have durations of $m_a$ and $m_b$, respectively. By selecting appropriate delays $d_a$ and $d_b$, rise time and flat top settings and using a linear combination of these two shapes, various WF can be synthesized.

The impulse responses of the CONCAVE and the CONVEX filters are ($h_a(j)$ and $h_b(j)$), respectively. Both responses are time limited. In general, the rise and the fall portions of the impulse responses $h_a(j)$ and $h_b(j)$ can be expressed as

$$\text{Rise} = \sum_{n=0}^{N} w_{a(b)}\, j^n \tag{1}$$

$$\text{Fall} = \sum_{n=0}^{N} w_{a(b)}\, (2k_{a(b)} + m_{a(b)} - j)^n \tag{2}$$

where $n = 0, 1, \ldots, N$; $j$ is the sample index.

The CONCAVE and CONVEX shapes have the same sign of their first ${}^1h_a(j)$ and ${}^1h_b(j)$ derivatives.

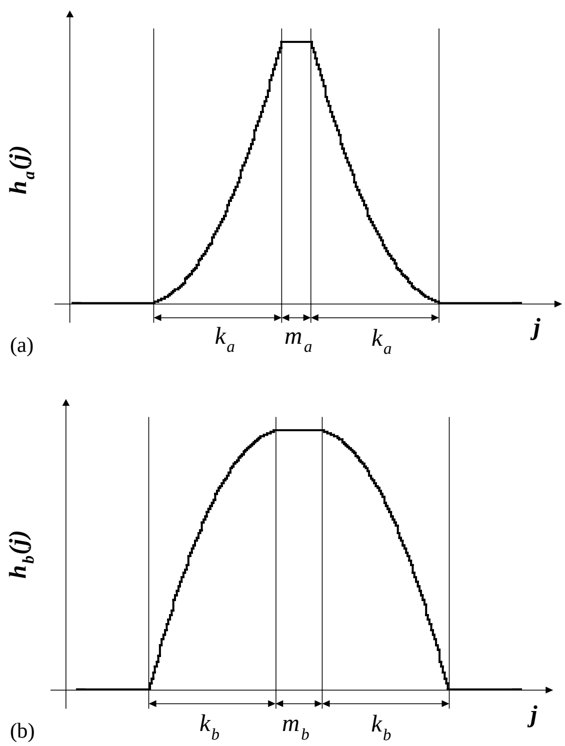


Fig. 2. Impulse responses: (a) CONCAVE, (b) CONVEX.

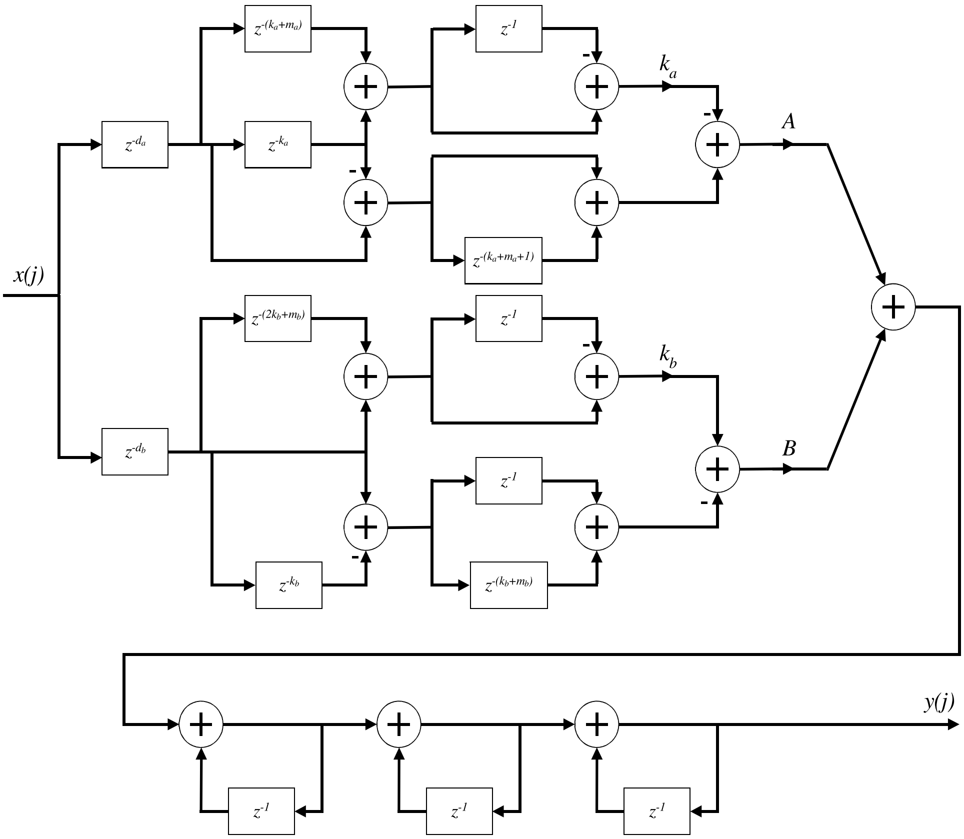


Fig. 3. Block diagram of the digital shaper with VWF. Shown are the impulse response equations of the CONCAVE and CONVEX filters:

$$h_a(j) = \begin{cases} 0 & j \leqslant 0 \\ \dfrac{j^2 + j}{2} & 0 < \mathrm{j} < k_b \\ \dfrac{k_a(k_a+1)}{2} & k_a \leqslant j \leqslant k_a + m_a \\ \dfrac{(2k_a + m_a - j)^2(2k_a + m - j)}{2} & k_a + m_a < j < 2k_a + m_a \\ 0 & j \geqslant 2k_a + m_a \end{cases}$$

$$h_b(j) = \begin{cases} 0 & j \leqslant 0 \\ \dfrac{2(k_b+1)j - j^2}{2} & 0 < \mathrm{j} < k_b \\ \dfrac{k_b(k_b+1)}{2} & k_b \leqslant j \leqslant k_b + m_b \\ \dfrac{(2k_b+1)(2k_b + m_b - j) - (2k_b + m_b - j)^2}{2} & k_b + m_b < j < 2k_b + m_b \\ 0 & j \geqslant 2k_b + m_b. \end{cases}$$

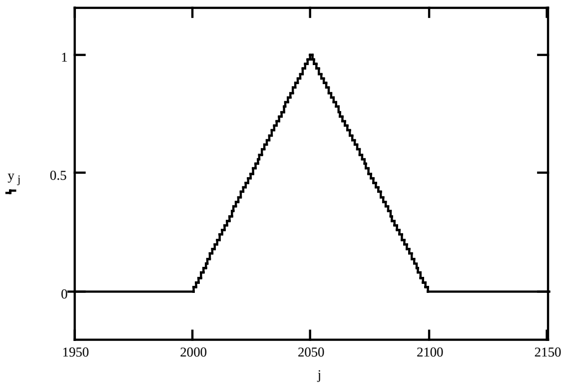


Fig. 4. Triangular shape. VWF parameters: $k_a = 50$, $m_a = 0$, $k_b = 50$, $m_b = 0$, $A = 1$, $B = 1$, $d_a = 0$, $d_b = 0$.

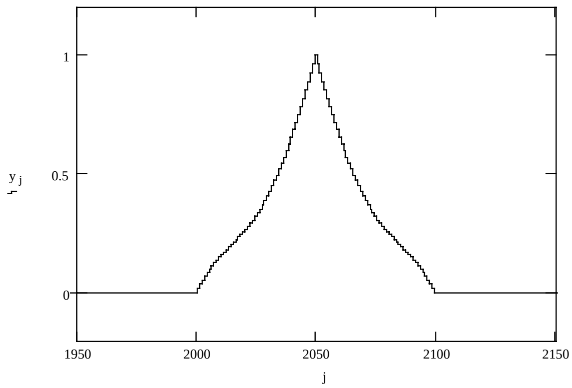


Fig. 5. Voltage $1/f$ noise shape [5]. VWF parameters: $k_a = 40$, $m_a = 0$, $k_b = 20$, $m_b = 60$, $A = 1$, $B = 1$, $d_a = 10$, $d_b = 0$.

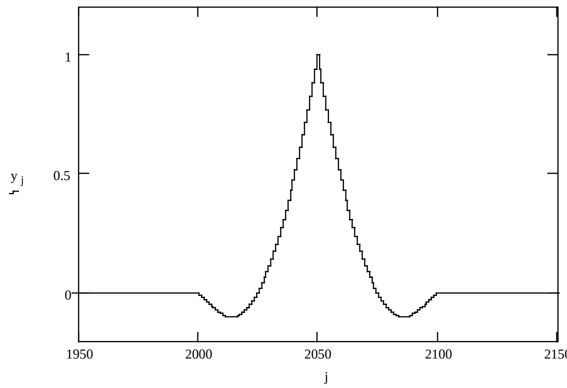


Fig. 6. Current $1/f$ noise shape [6]. VWF parameters: $k_a = 40$, $m_a = 0$, $k_b = 50$, $m_b = 0$, $A = 8$, $B = -1$, $d_a = 10$, $d_b = 0$.

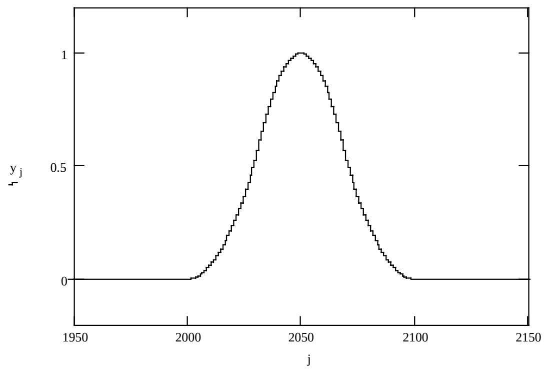


Fig. 7. Symmetric Quasi-Gaussian shape. VWF parameters: $k_a = 30$, $m_a = 40$, $k_b = 20$, $m_b = 0$, $A = 1$, $B = 2$, $d_a = 0$, $d_b = 30$.

The difference is in the sign of the second ${}^2h_a(j)$ and ${}^2h_b(j)$ derivatives

$$
\begin{aligned}
{}^1h_a(j) &= \begin{cases} >0 & \text{for } 0 < j < k_a \\ <0 & \text{for } k_a + m_a < j < 2k_a + m_a \end{cases} \\
{}^2h_a(j) &= \begin{cases} >0 & \text{for } 0 < j < k_a \\ >0 & \text{for } k_a + m_a < j < 2k_a + m_a. \end{cases}
\end{aligned} \tag{3}
$$

$$
\begin{aligned}
{}^1h_b(j) &= \begin{cases} >0 & \text{for } 0 < j < k_b \\ <0 & \text{for } k_b + m_b < j < 2k_b + m_b \end{cases} \\
{}^2h_b(j) &= \begin{cases} <0 & \text{for } 0 < j < k_b \\ <0 & \text{for } k_b + m_b < j < 2k_b + m_b \end{cases}
\end{aligned} \tag{4}
$$

Eqs. (1)–(4) are generalized descriptions of the waveforms of Fig. 2. A second-order CONCAVE and CONVEX filters are more practical for real time synthesis. A block diagram of the VWF filter realization and the impulse response equations of the CONCAVE and CONVEX filters are shown in Fig. 3. The filter was implemented in a programmable logic chip allowing operation at sampling clock up to 50 MHz.

## 3. Pulse shapes

To illustrate the ability of the VWF shaper a number of shapes were synthesized. Due to the limited space only few examples are shown. These shapes are depicted in Figs. 4–7.

## 4. Conclusion

Real time digital pulse shaping technique was developed that allows adjustment of the WF. By varying the WF efficient noise suppression can be achieved at various noise distributions. Efficient recursive algorithms were developed suitable for implementation in programmable logic.

## Acknowledgements

I would like to thank Randy Shepard from Canberra Industries for his support. The author appreciates the technical assistance of Dave Hall and Mat Kastner from the engineering division of Canberra Industries. I also thank professor Emilio Gatti from Politecnico di Milano for the helpful discussions.

## References

[1] V.T. Jordanov, et al., Nucl. Instr. and Meth. A 353 (1994) 261.
[2] G. Ripamonti, et al., Nucl. Instr. and Meth. A 340 (1994) 584.
[3] V. Radeka, IEEE Trans. Nucl. Sci. NS-15 (1968) 455.
[4] F.S. Goulding, Nucl. Instr. and Meth. A 100 (1972) 493.
[5] E. Gatti, M. Sampietro, Nucl. Instr. and Meth. A 287 (1990) 513.
[6] E. Gatti, et al., Nucl. Instr. and Meth. A 394 (1997) 268.
[7] V.T. Jordanov, Nucl. Instr. and Meth. A 351 (1994) 592.